



# Mechanical Properties of Hybrid Rice Straw Fibre and Walnut Shell ASH Particulate/Epoxy Composite

Chilee Ekwedigwe, Chidume Nwambu \*, Francis Osakwe, Eugene Nnuka

Department of Metallurgical and Materials Engineering, Faculty of Engineering, Nnamdi Azikiwe University, Awka Anambra State, Nigeria.

\*Corresponding author: Chidume Nwambu; [cn.nwambu@unizik.edu.ng](mailto:cn.nwambu@unizik.edu.ng)

Received 01 December 2022;

Accepted 10 January 2023;

Published 16 January 2023

## Abstract

This study focused on the effects of rice straw fibre and walnut shell ash particulates on the flexural and fatigue strength of epoxy composites. Conventional hand-lay-up techniques in five different weight proportions (i.e 2 wt.%, 4wt.%, 6wt.%, 8wt.% and 10wt.%) were used to reinforce the epoxy composites. The rice straw fibres were used to reinforce the epoxy composite separately, while rice straw fibres (RS<sub>f</sub>) combined with walnut shell ash particulates (WSA<sub>p</sub>) at an equal ratio were also used to reinforce the composites. The short beam shear tests were performed on the composites samples at room temperature to evaluate the flexural strength (according to ASTM D2344) and fatigue test. Both strengths were positively affected by reinforcement of the epoxy composites with rice straw fibre and walnut shell ash particulate. The presence of RS<sub>f</sub> and WSA<sub>p</sub> in the epoxy had great influences that altered the number of cycles obtained for the composite and shifted the cycle of failure to higher number. Amongst the different weight proportions, 6wt% of hybrid composite (rice straw fibre and walnut shell ash particulate) gave the highest flexural strength. A sustainable, affordable, and environmentally friendly alternative material for automotive, structural, and defense applications could be created with these epoxy biocomposites, which have improved mechanical properties.

**Keywords:** Composite, epoxy resin, rice straw, walnut shell ash particulate, flexural and fatigue strength.

## 1. Introduction

As the circular economy gains momentum, slogans like responsible waste management and designing for recycling are increasingly seen as equated with sustainable development. Over the past few years, the European Union has been moving increasingly towards circular economy, which means recycling, reusing and reducing materials as much as possible, Sydow et al. (2021). This aims to prevent waste entirely or to transform it into high-quality second-hand materials that profit from a market for second-hand raw materials that works well. The new Circular Economy Action Plan was adopted by the European Commission on 11 March 2020. In order to design such materials with the use of waste, scientists are increasingly focusing on agricultural (for example, natural fibers), industrial (for example, fly ash, red mud) or post-consumer (such as polymer bags, clothes) waste materials. Waste materials may be used as fillers or reinforcements in metal or polymer-based composites suited for various applications, e.g., tribological materials relating to friction-induced wear.

In light of these requirements, long fibre reinforced polymer composites proffer an ideal solution since they have high specific strength, high stiffness, corrosion resistance, and low density, Rabbani et al., (2022), Bisht et al., (2020). Although glass and carbon fibre are the primary reinforcement materials for composites, Nwambu et al. (2022). Natural fibres can also serve as a

reinforcement material for epoxy composite, Kuram (2020) Yadav et al., (2021). As a result of their inherent superior properties, synthetic fibre-reinforced polymer composites have been incorporated into a wide range of applications, including the construction, aerospace, and automobile industries, Nwambu et al., (2022), Ibrahim et al., (2010). However, these composites are non-biodegradable, which poses a significant threat to the ecological system, Braga et al., (2015). In addition, synthetic fibres, such as glass and carbon, pose several health risks. The need for lightweight materials coupled with strict environmental rules and regulations have led to the development of natural fibre reinforced biocomposite materials, Arifuzzaman-Khan et al., (2016).

Several researchers have investigated the effect of natural fibres on the mechanical properties of the epoxy composite. For example, Rabbani et al., (2022) characterised the mechanical properties of the biocomposite by using the polypropylene random copolymer (PPRC), and biowaste rice husk (BRH) as the primary raw materials. They found that the modulus and hardness of the biocomposite improved by 44.8% and 54.8% due to the neat PPRC, respectively. Also, Kuram (2020), studied the effect of natural filler on the morphological, rheological and mechanical properties of acrylonitrile-butadiene-styrene (ABS) terpolymer. The powdered hazelnut and walnut shells were employed as natural filler with ABS to develop hybrid polymer composites. Their findings revealed that the highest strengths and flexural modulus were achieved with 5wt%

of hazelnut and 15wt% of walnut shell four among all hybrid composites. Bisht *et al.*, (2020) attempt to understand the applicability of rice husk as a fibre with various polymers composites. They highlighted various modification techniques that can enhance the mechanical properties of biocomposite reinforced with rice husks by altering their chemical and physical properties. Yadav *et al.* (2021) proposed that utilising various weight percentages of rice husk ash and eggshell as reinforcement material with aluminum can improve the mechanical properties of composites.

These natural fibres are rice straw and walnut shell ash. Rice straw, as a lignocellulosic biomass, comprises three components: lignin, cellulose, and hemicelluloses. These could be fractionated through pretreatment, Saidah *et al.*, (2017). Walnut shell is a waste generated in the walnut (*tetracarpidium conophorum*) harvest, containing natural antioxidant compounds such as flavonoids, Akbari *et al.*, (2012). Much environmental pollution is involved in disposing of these natural fibres, kuram (2020). Thus, it is necessary to find new ways to use these natural fibres which will prevent environmental concerns and provide a second income for farmers, Okafor *et al.*, (2022). The purpose of this paper is to enhance the mechanical properties of epoxy composites using rice straw fibre and walnut shell ash particulate reinforcement.

## 2.0 Material and methods

### 2.1 Materials

The experiments were conducted with epoxy (LY556) bisphenol-A-diglycidyl-ether, hardener (HY-951), sodium hydroxide solution and acetic acid solution obtained from Lagos. Rice straw fibres and walnut shells were obtained from Abakiliki, Ebonyi state. At the same time, petroleum jelly and distilled water were from the Chemistry Department, University of Nigeria, Nsukka. All the equipment used in the experiment are as follows; vibratory sieve shaker, electric oven, weighing balance, universal material testing machine Cat Nr. model:261 and SEM machine model: JEOL JSM840.

### 2.2 Chemical treatment of bio fibres

Rice straw fibres (RSf) were washed with regular water to remove dirt and air-dried at 25-30°C for 24 hrs and were treated with NaOH to improve the quality. Likewise, the walnut shell (WSAp) was washed, dried, and placed inside a perforated cylinder pan for combustion into ash. The obtained ash was then placed inside an alumina crucible, put inside a muffle furnace, heated to a temperature of 900°C and held for 5hrs to reduce the carbonaceous matter and increase the percentage of active silica content. The X-ray diffraction patterns of the WSAp and RSf was determined by Siemens D-500 diffractometer using Co-K $\alpha$  radiation (K $\alpha$  = 1.79026 Å). The microscopic study of WSAp and RSf was determined by JEOL JSM840A scanning electron microscope (SEM) complemented by EDS. Particle size and morphology of produced WSAp were examined by TEM (Jeol, JSM2010), using a 200 keV electron beam on the sample mounted on a carbon-coated copper grid. The WSAp was a suspension taken using a dropper, spread on the carbon coated copper grid, and allowed to dry at room temperature. The copper grid was introduced into the instrument, and the sample chamber was evacuated. The sample was scanned along the path of the electron beam, and a photograph of the sample was taken. The elemental composition of the WSAp and RSf were determined by X-Ray Fluorescence (XRF) analysis. The samples were formed into pellets in a pelletiser with the hydraulic press (Carver Inc). The pellets were sealed at the chamber of the XRF

(Amptek Inc) and allowed to run for 1000s at a voltage of 20 kV, and a current of 40 $\mu$ A.

### 2.3 Manufacturing procedure

Rice straw fibre (RSf) reinforced epoxy resin composites were fabricated by conventional hand-lay-up techniques in five different weight proportions (i.e 2 wt.%, 4wt.%, 6wt.%, 8wt.% and 10wt.%), while the hybrid composites were measured at the equal ratio of rice straw fibre (RSf) to walnut shell ash particulate (WSAp) and produced in five different weight proportions (i.e 2 wt.%, 4wt.%, 6wt.%, 8wt.% and 10wt.%). The WSAp was thoroughly dispersed in the matrix material using Digital Sonicator (Q-700-200, Qsonica, Newton, USA)) for homogeneity concerns. The low temperature curing epoxy resin and corresponding hardener were blended in a ratio of 10: 1 by weight as recommended by the supplier and available literature, Debnath *et al.*, (2013). The mixing was done meticulously before the rice straw fibre mats were reinforced in the matrix body. Fibre mats were cut in the dimension of 400mm  $\times$  400mm, and the wooden mould of 410  $\times$  410  $\times$  40 mm<sup>3</sup> was used to fabricate the composites. The composite slabs were fabricated by a modified hand lay-up method followed by a light compression moulding technique. After curing, easy release of composite from mould was assured by applying releasing agent (Silicon spray). Care was taken for WSAp powder-filled epoxy composites to ensure a uniform sample since solid particles tend to clump and tangle together when mixed. The curing of composites took place under a load of 25 kg for 24 hours before removal from the mould. Then, the composite slabs were post-cured in the air for another 24 hours after removal from the mould. For testing, specimens of the size specified by respective standards were cut from the prepared composite slabs using a diamond cutter. Homogeneity of the composite were maintained with the utmost care during fabrication.

### 2.4 Mechanical characterization

#### 2.4.1 Flexural strength

The short beam shear (SBS) tests were performed on the composite samples at room temperature to evaluate the flexural strength. It is a 3- point bend test, which generally promotes failure by inter-laminar shear. The SBS test was conducted as per ASTM standard (D2344) using the Testometric testing machine same as used for tensile testing. The dimension of the specimen was 40 mm  $\times$  10 mm  $\times$  (4) mm and test were conduct at crosshead speed of 10mm/min. The flexural strength and flexural modulus of specimen were calculated using equations 1 and 2 respectively. The inter-laminar shear strength (ILSS) was determined using following equation. 3 (Patnaik *et al.*, 2009).

$$FS = \frac{3PL}{2bt^2} \text{-----} 1$$

$$FM = L^3 M / 4bt^3 \text{-----} 2$$

$$ILSS = \frac{3P}{4bt} \text{-----} 3$$

Where, P is maximum applied load, L the span length of the sample, m – slope of tangent, b the width of specimen, t the thickness of specimen.

#### 2.4.2 Fatigue Test

Two servo-hydraulic test benches 220 kN Zwick/Roel test frame and a custom-built 100 kN test frame were used. Temperature control

was provided by a climate chamber annexed to the test frames and piped to an isolated box surrounding the grips and specimen. Conditioned air was circulated through the system, and the settings of the external climate chamber were adjusted based on temperature measurements in the test area. Relative humidity was not controlled. The room temperature tests were typically not carried out in the climate chamber but only under laboratory conditions. For low and high temperature tests, specimens were left to stabilize at the desired temperature for at least 15 minutes, or until measured specimen temperature was within one degree centigrade of the target environment. Static tests were carried out in displacement control and fatigue tests were load controlled. Fatigue experiments were load controlled and performed at  $R = -1$ , with  $R$  being defined as the ratio of the minimum stress during the cycle ( $S_{min}$ ) over the maximum cyclic stress ( $S_{max}$ ) according to equation 4.

$$R = \frac{S_{min}}{S_{max}} \tag{4}$$

Therefore,  $R = 0.1$  makes for a pure tensile fatigue case and  $R = -1$  implies a fully reversed fatigue cycle with an equal tensile and compressive stress magnitude. All  $S-N$  curves and their equations were based on the maximum stress  $S_{max}$ , or the maximum stress normalized by the static strength at the test temperature  $S_{max}/S_{st}$ . Note that a capital  $S$  denotes a strength while a lower-case  $s$  is used for stress. In practice, a maximum cyclic load  $P_{max}$  was defined, and the stress was calculated according to equation 5.

$$S = \frac{P_{max}}{A} \tag{5}$$

### 3.0 Results and Discussions

#### 3.1 Flexural Strength of the Composites

The flexural modulus and flexural strength are shown in Figures 1 and 2. In Figures 1 and 2, it was observed that the flexural modulus and flexural strength of the reinforced composites were improved, when compared with the composite samples with pure polymer epoxy. The improvement in flexural strength and modulus could be attributed to the high stiffness and toughness of the hybrid composites (epoxy-RSf+WSA<sub>p</sub>) which helped to strengthen the materials under bending forces. Also, better interfacial adhesion between matrix and reinforcements which improved stress transfer from matrix to reinforcement resulting to higher values of flexural strength. Weak fiber/matrix interfacial bonding may result to poor flexural properties. The results aligned with the force versus displacement deflection curves. The composites with epoxy/RSf have a large area under the curves, while that of the epoxy/RSf+WSA<sub>p</sub> have a large area under the force versus displacement deflection to maximum at 6wt percent of epoxy/RSf+WSA<sub>p</sub>. Beyond 6 percent of epoxy/RSf+WSA<sub>p</sub> addition, the hard nature of the WSA<sub>p</sub> helped to decrease the flexural strength.

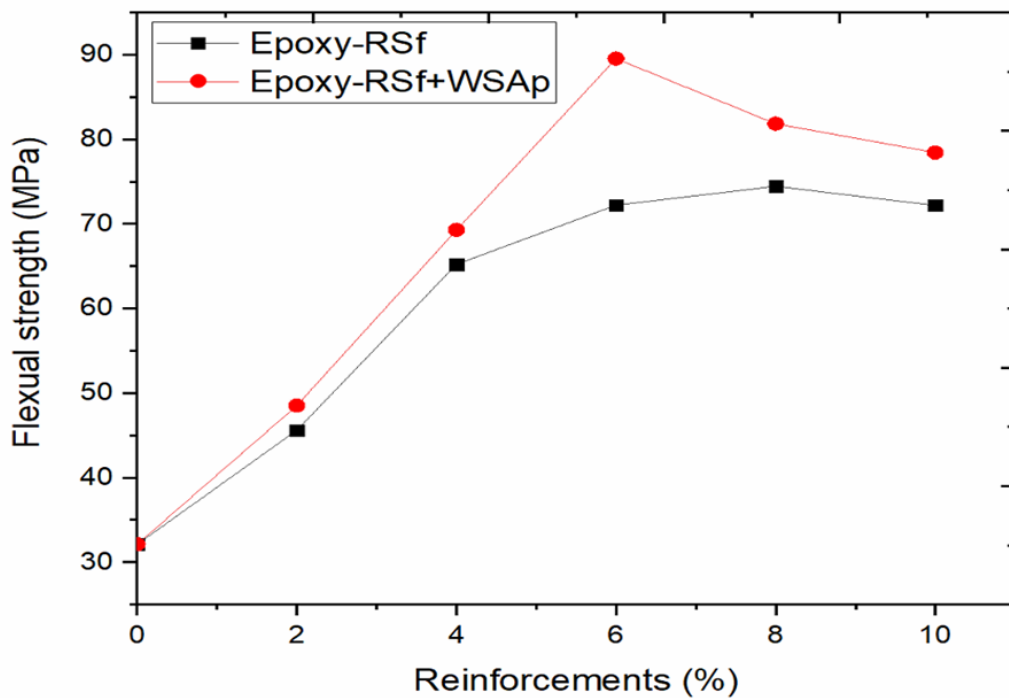


Figure 1: Effect of the reinforcements on the flexural strength of the composites

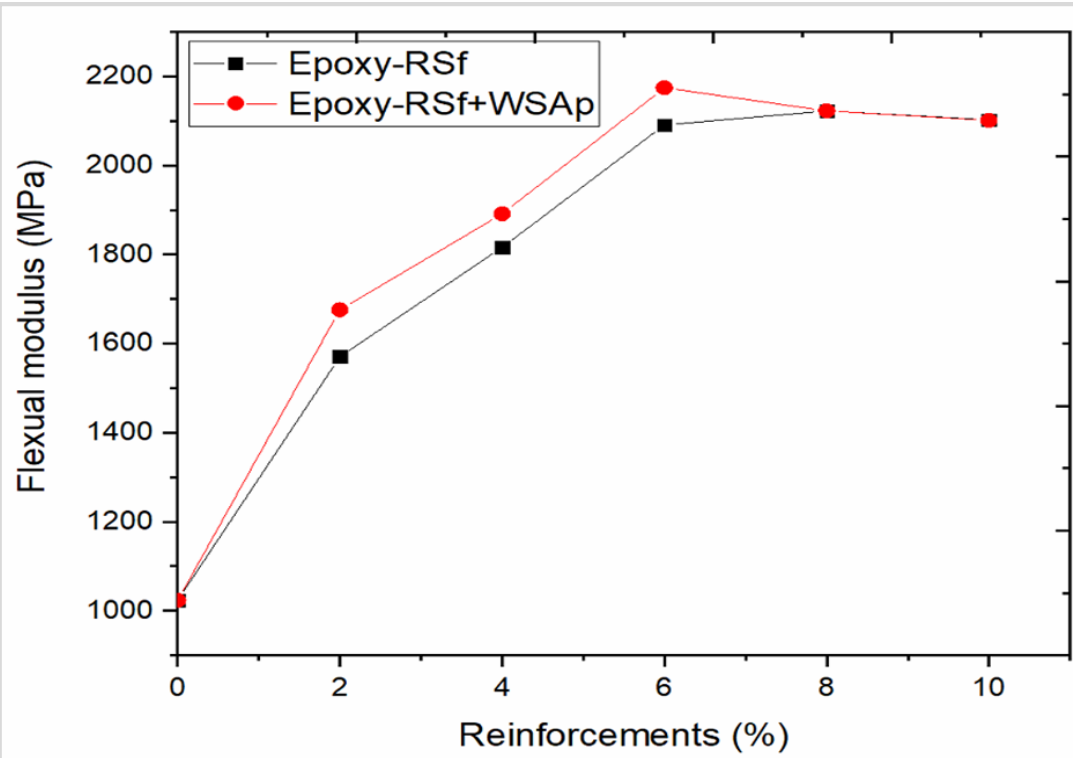


Figure 2: Effect of the reinforcements on the flexural modulus of the composites.

For the epoxy/ $RS_f$  composites the flexural strength increased with increase in weight percent of rice straw fibres ( $RS_f$ ) from 2 to 8 before decrease. Percentage improvement of 173.66% and 182.84% over that of the pure epoxy were obtained at 8 percent of epoxy/wt% $RS_f$  and 6 percent of epoxy/ $RS_f$ + $WSA_p$  composites respectively.

**3.2 Fatigue strength of the composites.**

Fatigue property is an important factor in the design of wind turbine blade due to the cycling motion of the operation of the wind turbine.

Figure 3 presents the stress versus number of cycles(S-N) obtained during the fatigue investigation of the composite samples. The stress versus number of cycles of the composite was different from that of the epoxy matrix (Figure 3). The epoxy- $RS_f$  and epoxy- $RS_f$ +  $WSA_p$  composites had a higher number of cycles before failure than the matrix. The presence of  $RS_f$  and  $WSA_p$  in the epoxy had great influences that altered the number of cycles obtained for the composite and shifted the cycle of failure to higher number. The high modulus obtained for the composites was the major reason for the enhancement of the fatigue strength.

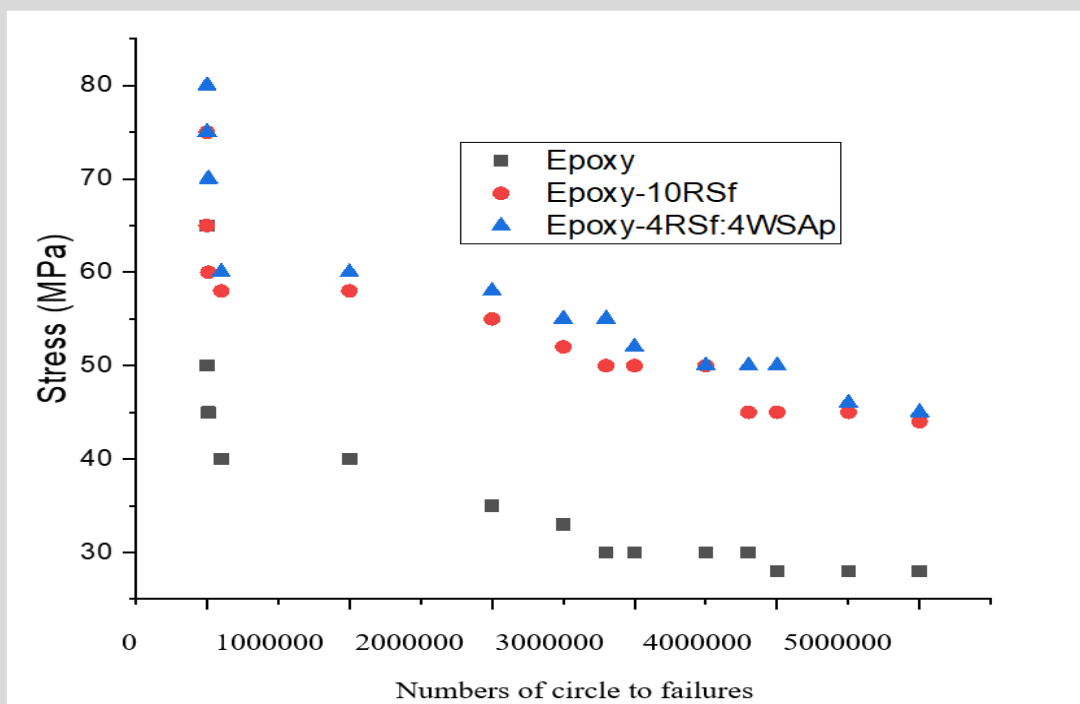


Figure 3: Representative of stress against the numbers of circle to failures of the composites

At the same stress level of 60MPa the number of cycles to failures were: 1000, 1000000 and 1100000 for the epoxy, epoxy- $RS_f$  and epoxy- $RS_f$ +  $WSA_p$  composites respectively. The higher number of

cycles of fatigue obtained for the epoxy- $RS_f$ +  $WSA_p$  composite was attributed to the presence of  $SiO_2$  and  $Al_2O_3$  which resisted the easy movement of the polymer chains. Also increases in fatigue strength

was attributed to the reduction in both the elastic and plastics strains which arose from increasing modulus and work hardening effect.

In Figure 3 it was seen that the fatigue strength of the matrix increased from 35.00 to 55.0MPa and 35.00 to 60.00MPa, epoxy-RS<sub>f</sub> and epoxy-RS<sub>f</sub>+WSA<sub>p</sub> composites respectively. This represents 57.14 and 71.43% improvement of the fatigue strength of the matrix.

### 3.3 Fracture surface of the tensile sample

Figures 4-6 displayed the tensile fracture surface and showed a significant difference in fracture morphology of the samples under investigation. The fracture surface of the 100%epoxy with reinforcement showed a coarse and zig-zag surface (Figure 4). This was due to the brittle nature of the surface.

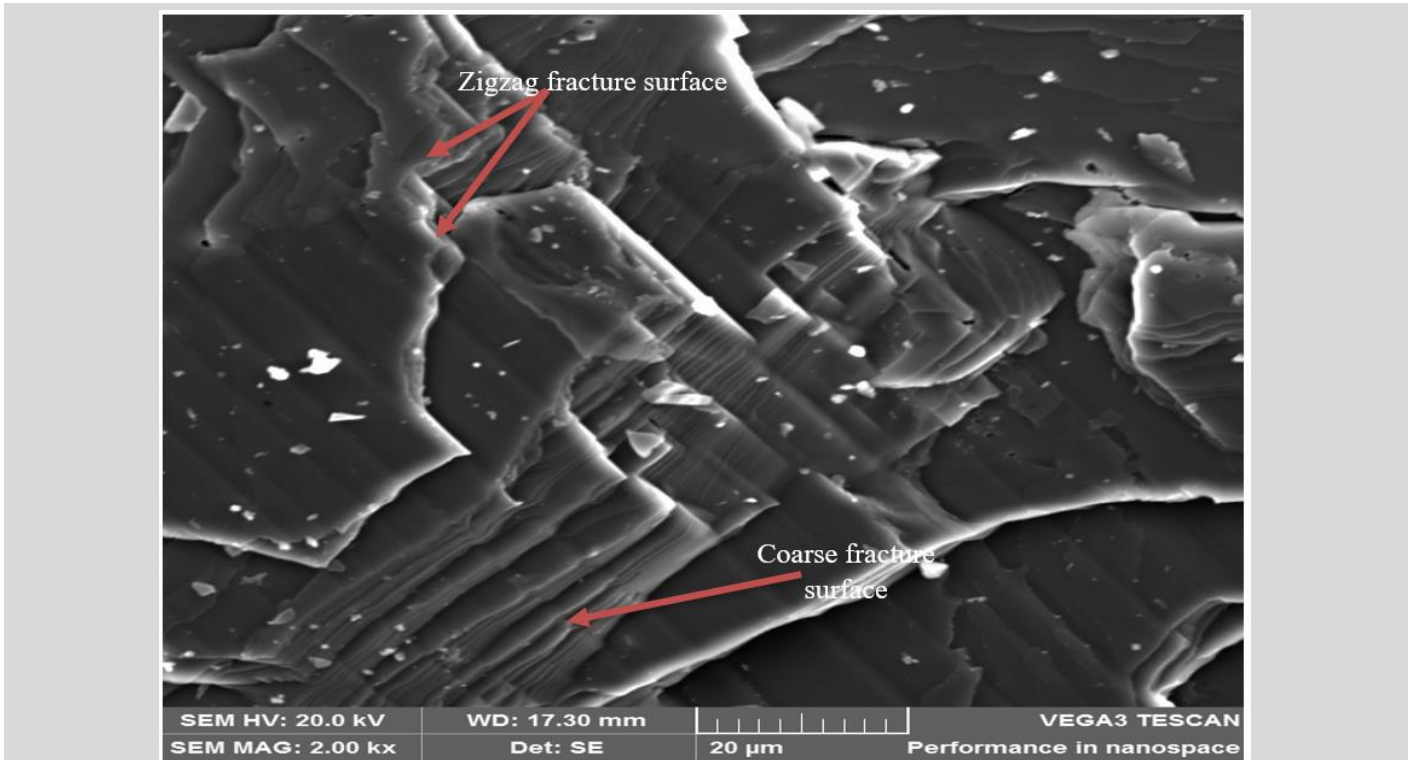


Figure 4: SEM tensile fracture surface of the composite sample with 100%epoxy.

The tensile fracture surface of the composites showed that the reinforcement was covered with epoxy. This could be attributed to good interfacial bonding between the reinforcement and the epoxy. This was the major reason why the tensile strength obtained in the reinforcement composites was higher than that of the pure epoxy composited under investigation. A similar observation of

improvement in tensile strength of epoxy after reinforcement was reported by Nwambu *et al.*, (2022). However, when Figure 4 was compared to Figure 6, it became clear that there were some particle detachments from the epoxy-RS<sub>f</sub>+WSA<sub>p</sub> composites. These particle detachments were the reason behind the optimum tensile strength obtained in 6wt% of epoxy-RS<sub>f</sub>+WSA<sub>p</sub>.

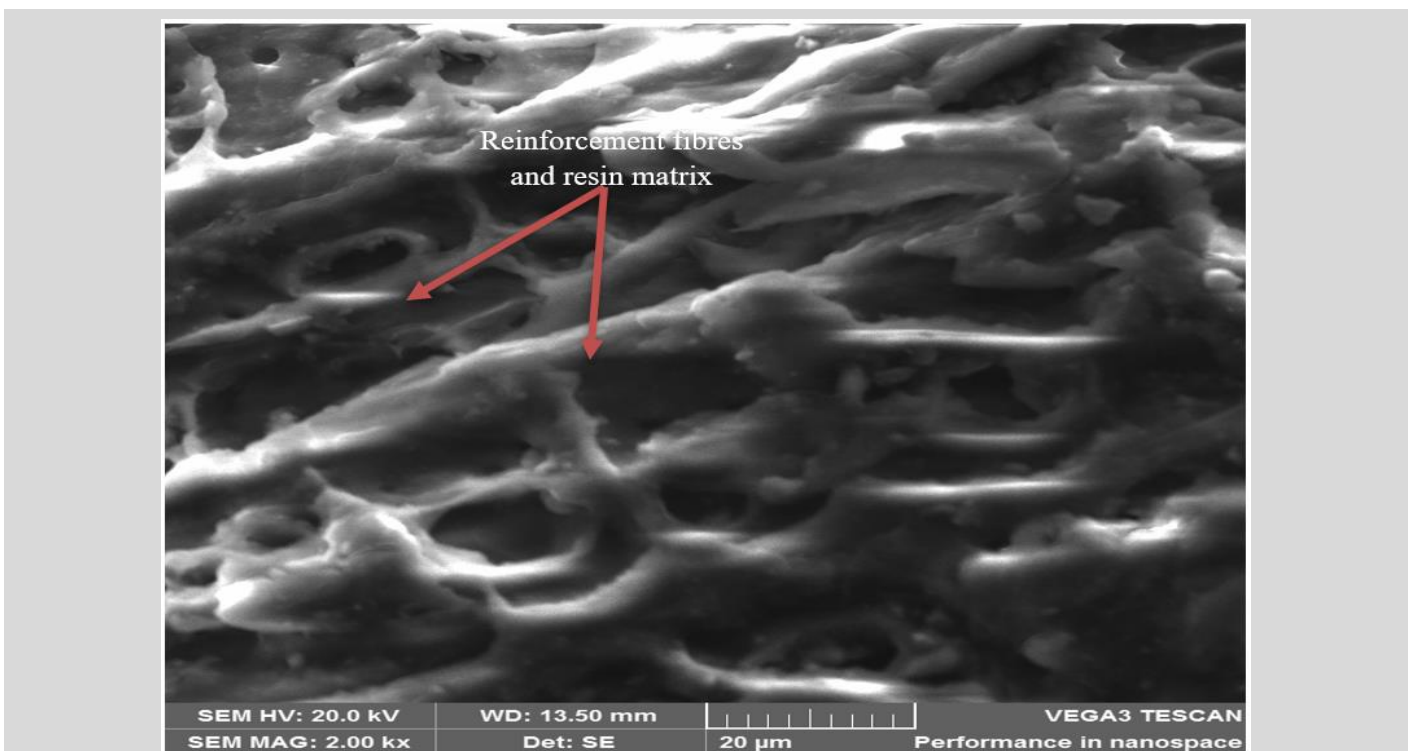


Figure 5: SEM tensile fracture surface of the composite sample with epoxy-8wt%RS<sub>f</sub>.



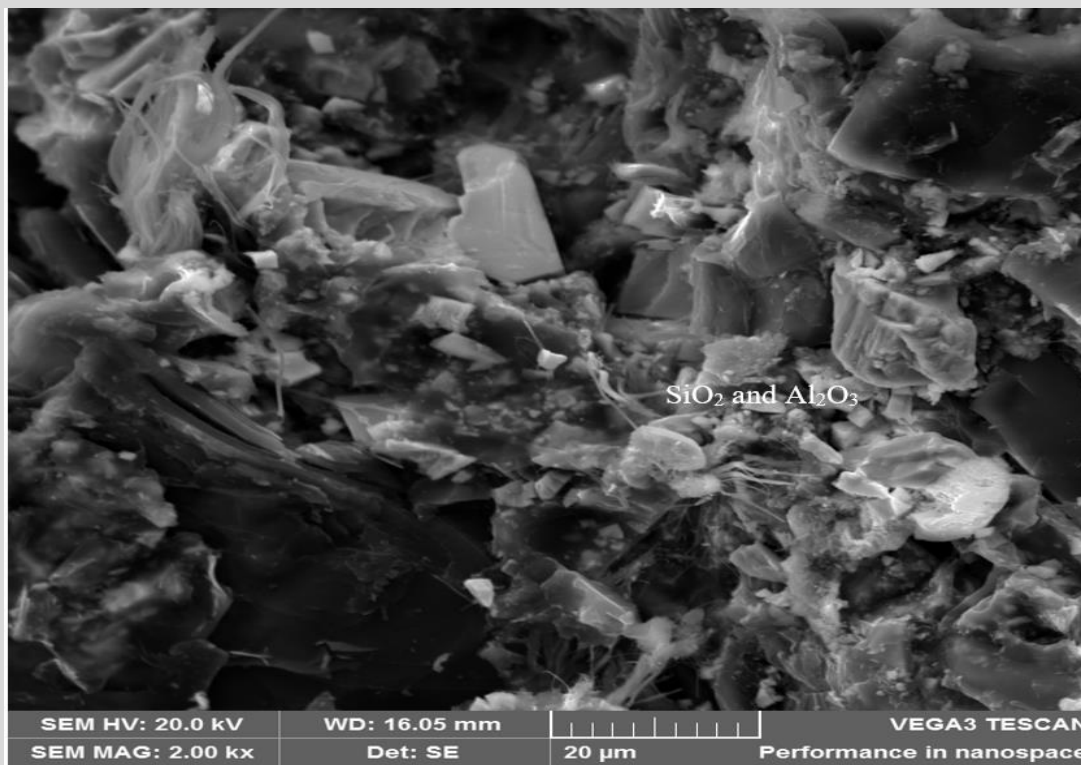


Figure 6: SEM tensile fracture surface of the composite sample with 6wt% of epoxy-RSf+WSAp.

This study may offer valuable insights into selecting the best material during production to enhance the performance of tidal turbine blades and automotive equipment in the future. In order to gain a complete understanding of the relationship between the microstructure and the mechanical behavior of particulate reinforced composites, the tensile and impact strength of the epoxy composite were investigated. Based on the analysis of the bio-fibres as reinforcement materials on the epoxy composite for improvement of mechanical properties, bio-fibres could be selected for use in eco-friendly composite construction. The findings of this research align with the reports of recent studies, Saidah *et al.*, (2017), Okafor *et al.*, (2022), Nwambu *et al.*, (2022) on the effects of bio-fibres on the mechanical behaviors of epoxy composite structures.

#### 4.0. Conclusion

As a result of the reinforcements (rice straw fibre and walnut shell ash particulate), the composite showed improved mechanical properties. The improved flexural strength obtained at 8wt% of RSf and 6wt% of RSf+WSAp is within the recommended. Improvement of fatigue energy were obtained at 8wt% of epoxy-RSf and 6wt% of epoxy-RSf+WSAp composites. The hybrid composite samples can absorb and dissipate energy better at 8wt% of epoxy-RSf and 6wt% of epoxy-RSf+WSAp. A sustainable, affordable, and environmentally friendly alternative material for automotive, structural, and defense applications could be created with these epoxy biocomposites, which have improved properties.

#### Statement of Completing interest

The authors declaration of no conflict of interest

#### List of Abbreviations

RSf: Rice straw fibre  
 WSAp: Walnut straw ash particulate  
 SEM: Scanning electron microscope

#### References

- [1] Abas F.O., R.O. Abas, S.I. Ibrahim, A Comparison Study of Different Ceramic Filler on Mechanical and Thermal Properties of Glass, Carbon, Kevlar / Polyester Composites, *Engineering & Technology Journal*, 28 (2010) 2469-2479.
- [2] Ibrahim, I. S., Abas, R. O. and Abas F.O. (2010); A Comparison study of different ceramic filler on mechanical and thermal properties of glass, carbon, kevlar / polyester composites; *Engineering & Technology Journal*, Vol. 28 No. 12 pp. 2469-2479.
- [3] Arifuzzaman-Khan, G. M., Terano, M., Gafur, M. A. and Shamsul-Alam, M. (2016); Studies on the mechanical properties of woven jute fabric reinforced poly (L-lactic acid) composites; *Journal of King Saud University – Engineering Sciences* 28 (2016) 69–74.
- [4] Alshahrani, H. and Prakash, A. (2022); Mechanical, wear, and fatigue behaviour of alkali-silane-treated areca fiber, RHA biochar, and cardanol oil-toughened epoxy biocomposite; *Biomass Conversion and Biorefinery*.
- [5] Abdul-Nasir, A. A., Azmi, A. I. and Khalil, A. N. M. (2014); Investigating the effect of machining parameters on mechanical performance of Flax Natural Fibre Composites with Circular Holes; *Conference: Advances in Material Processing Technologies*.
- [6] Andi Saidah, Yudinata, Sri Endah Susilowati, Saidah, A. and Susilowati, S. E. (2017) Design of composite material of rice straw fiber reinforced epoxy for automotive bumper, 2017 International Conference on Computing, Engineering, and Design (ICCED). Pp. 1-4.
- [7] Akbari, V., Jamei R., Heidari, R. and Esfahlan, A. J. (2012); Antiradical activity of different parts of Walnut (*Juglansregia L.*) fruit as a function of genotype; *Food Chemistry*; Vol. 135 No. 4 pp. 2404-2410.
- [8] Braga, R. A. and Magalhaes Jr P. A. (2015); Analysis of the mechanical and thermal properties of jute and glass

- fiber as reinforcement epoxy hybrid composites; *Materials Science and Engineering*, Vol. 56 pp. 269–273.
- [9] Nwambu C N, Robert C and Alam P 2022 The tensile behaviour of unaged and hygrothermally aged asymmetric helicoidally stacked CFRP composites *J.Compos. Sci.* 6 137
- [10] Chandrasekaran, S., Sato, N., Tolle, F., Mulhaupt, R., Fiedler, B. and Schulte, K. (2014); Fracture toughness and failure mechanism of graphene-based epoxy Composites; *Composites Science and Technology*, Vol. 97 pp. 90–99.
- [11] Okafor, C. E., Kebodi, L. C., Kandasamy, J., May, M. and Ekengwu, I. E. (2022); Properties and performance index of natural fiber reinforced cross-ply composites made from *dioscorea alata* stem fibers; *Composites Part C*, Vol. 7 pp. 100213.
- [12] Debnath K., Singh, I., Dvivedi, A. and Kumar. P. (2013); Natural fibre reinforced-polymer composites for wind turbine blades: challenges and opportunities; *Recent Advances in Composite Materials for Wind Turbines Blades*, pp. 25-38.
- [13] Kuram, E. (2020); Rheological, mechanical and morphological properties of hybrid hazelnut (*corylus avellana* L.)/walnut (*Juglans regia* L.) shell four-filled acrylonitrile butadiene styrene composite; *Journal of Material Cycles and Waste Management*, Vol. 22 pp. 2107–2117.
- [14] Fahad Ali Rabbani, Saima Yasin, Tanveer Iqbal and Ujala Farooq Rabbani, F. A., Yasin, S., Iqbal, T. and Farooq, U. (2022); Experimental study of mechanical properties of polypropylene random copolymer and rice-husk-based biocomposite by using nanoindentation; *Materials*, Vol. 15 No. 5 pp. 1956.
- [15] Nwambu C, Robert C and Alam P 2022 Viscoelastic properties of bioinspired asymmetric helicoidal CFRP composites *MRS Adv.* (<https://doi.org/10.1557/s43580-022-00332-0>)
- [16] Nwambu C, Robert, C, and Alam, P. (2022). Dynamic mechanical thermal analysis of unaged and hygrothermally aged discontinuous asymmetric helicoidally structured CFRP composites. *Funct. Compos. Struct.* 4 045001.
- [17] Sydow Z, Sydow M, Wojciechowski L and Bienczak K. (2021) Tribological performance of composites reinforced with the Agricultural, industrial and post-consumer wastes: A review: *Materials* Vol. 14 No. 8 pp. 1863.



**Open Access** This article is licensed under a Creative Commons Attribution 4.0 International License, which permits use, sharing, adaptation, distribution and reproduction in any medium or format, as long as you give appropriate credit to the original author(s) and the source, provide a link to the Creative Commons license, and indicate if changes were made. The images or other third-party material in this article are included in the article's Creative Commons license, unless indicated otherwise in a credit line to the material. If material is not included in the article's Creative Commons license and your intended use is not permitted by statutory regulation or exceeds the permitted use, you will need to obtain permission directly from the copyright holder. To view a copy of this license, visit <https://creativecommons.org/licenses/by/4.0/>.

© The Author(s) 2023